Test Structures for Characterizing the Integration of EWOD and SAW Technologies for Microfluidics

Yifan Li, *Member, IEEE,* Richard Yongqing Fu, *Member, IEEE,* D. Winters, Brian W. Flynn, Bill Parkes, Douglas Stuart Brodie, Yufei Liu, Jonathan Terry, *Member, IEEE,* Les I. Haworth, A. S. Bunting, J. T. M. Stevenson, Stewart Smith, *Member, IEEE,* C. Logan Mackay, Pat R. R. Langridge-Smith, Adam A. Stokes, *Member, IEEE,* Anthony J. Walton, *Senior Member, IEEE*

***Abstract*—This paper presents details of the design and fabrication of test structures specifically designed for the characterization of two distinct digital microfluidic technologies: electro-wetting on dielectric (EWOD) and surface acoustic wave (SAW). A test chip has been fabricated that includes structures with a wide range of dimensions and provides the capability to characterize enhanced droplet manipulation, as well as other integrated functions. The EWOD and SAW devices have been separately characterized first of all to determine whether integration of the technologies affects their individual performance, including device lifetime evaluation. Microfluidic functions have then been demonstrated, including combined EWOD/SAW functions. In particular, this paper details the use of EWOD to anchor droplets, while SAW excitation is applied to perform mixing. The relationship between test structure designs and the droplets anchoring performance has been studied.**

***Index Terms*—Contact angle, electro-wetting on dielectric (EWOD), integration, surface acoustic wave (SAW), test structure.**

I. Introduction

DIGITAL microfluidic technologies, which involve the movement of fluidic samples in droplet form instead of continuous flow within a channel, include surface acoustic wave (SAW) and electro-wetting on dielectric (EWOD) [1]–[7]. As methods of manipulating fluids they both have their attractions, including simple electrode structures and potentially non-complex integration with CMOS integrated circuits and other electrode technologies, such as electrophoresis and dielectrophoresis.

Manuscript received October 14, 2010; revised January 13, 2012; accepted March 20, 2012. Date of publication June 5, 2012; date of current version July 31, 2012. This work was supported in part by the Edinburgh Research Partnership in Engineering and Mathematics, BBSRC, and EPSRC (RASOR Project BBC5115991), by the Carnegie Trust, by the European Community (GOLEM Project 033211), and by the Innovative Electronic Manufacturing Research Center through the EPSRC Funded Flagship Project SMART MICROSYSTEMS (FS/01/02/10).

Y. Li, D. Winters, B. W. Flynn, B. Parkes, J. Terry, L. I. Haworth, A. S. Bunting, J. T. M. Stevenson, S. Smith, C. L. Mackay, P. R. R. Langridge-Smith, A. A. Stokes, and A. J. Walton are with the University of Edinburgh, Edinburgh EH9 3JF, U.K. (e-mail: y.li@ed.ac.uk).

D. S. Brodie is with Heriot-Watt University, Edinburgh EH14 4AS, U.K.

Y. Liu is with the College of Engineering, Swansea University, Swansea SA2 8PP, U.K.

R. Y. Fu is with the Thin Film Centre, University of the West of Scotland, Paisley PA1 2BE, U.K. (e-mail: richard.fu@uws.ac.uk).

Color versions of one or more of the figures in this paper are available online at http://ieeexplore.ieee.org.

Digital Object Identifier 10.1109/TSM.2012.2202770

A. SAW Technology

SAW-based technology is relatively mature having been developed decades ago for radio-frequency (RF)-based signal processing and sensing devices. It uses RF signals to generate surface waves by applying an a.c. voltage to interdigitated electrodes on a piezoelectric substrate. This is shown schematically in Fig. 1(a), which also includes a second set of electrodes being used as a sensor capable of detecting the surface wave. The frequency of the SAW is determined by the electrode finger width, d [3], the width of a propagated wave is set by the interdigitated transducer (IDT) finger length, W, while the transmission amplitude depends on the number of finger pairs, N.

B. EWOD Technology

EWOD devices comprise a layer of metal, which forms the electrode, a dielectric, which insulates the electrode from the liquid, and a hydrophobic coating such as Teflon-AF or CYTOP on the top surface. When a DC voltage is applied to an EWOD electrode, the movement of charges to the liquid-dielectric interface modifies the surface from hydrophobic to hydrophilic. Droplets on the surface are attracted to the hydrophilic electrodes, which is illustrated schematically in Fig. 1(b). All the basic functions associated with the control of droplets, such as movement, positioning, merging and splitting, have been demonstrated [2], [4], [5] by programming appropriate electrode switching sequences.

C. SAW and EWOD Integration

As mentioned previously, both EWOD and SAW have specific advantages and integrating the two technologies is attractive as it can combine the best elements of each to create improved system functionality [1], [8]. For example, an integrated device has the potential to combine functions such as EWOD droplet positioning with SAW mixing and EWOD droplet transport with SAW sensing [1]. In addition, the surface switching capability of EWOD and SAW technologies can also be combined in order to dynamically guide droplets with more precision. The test structures reported in this paper have been developed to characterize the design, fabrication, and operation of devices that integrate the two technologies.

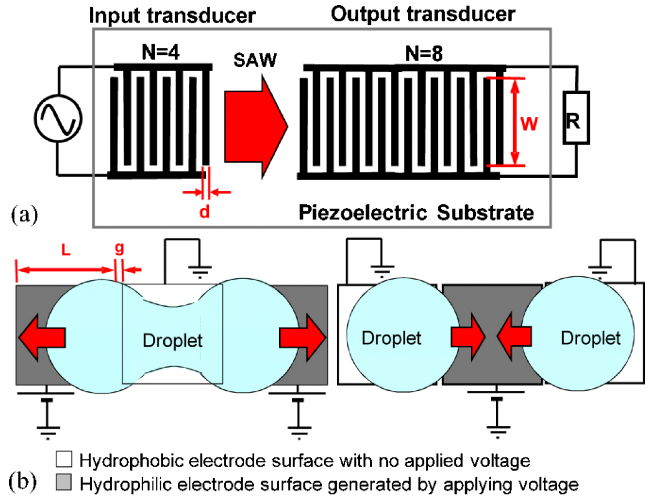

Fig. 1. (a) Schematic layout of SAW device showing the interdigitated finger structure of the electrodes. (b) EWOD device splitting and merging droplets by switching electrode hydrophobicity.

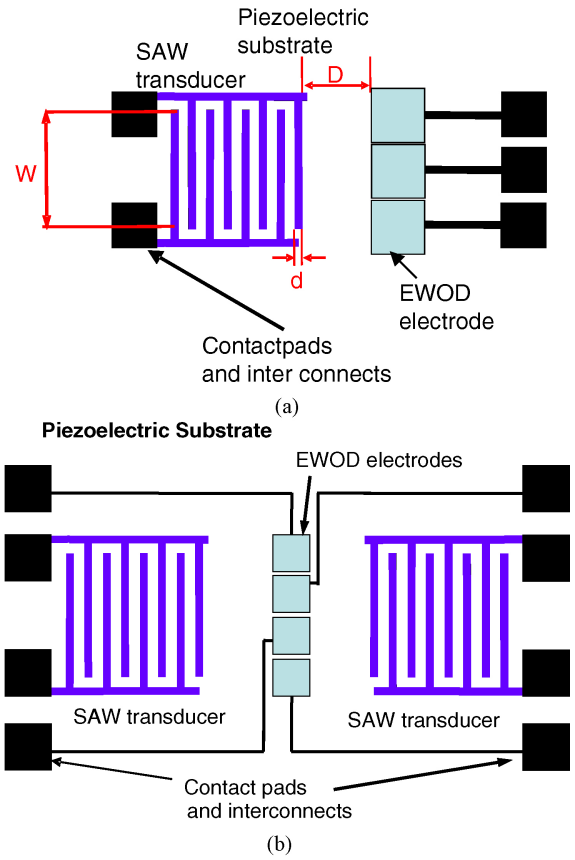

Fig. 2. Schematic showing integrated EWOD SAW test structures. (a) Three EWOD electrodes centered on the SAW axis. (b) Two SAW IDTs with four electrodes.

II. Test Structure Design Considerations

A. Test Structure Layout

Fig. 2(a) shows a schematic of an integrated test structure which was designed to evaluate the fabrication process parameters and materials, as well as to characterize basic EWOD and SAW devices working both independently and together. In this design, the EWOD electrode array is located in front of SAW interdigitated transducers so that droplets can be manipulated by either EWOD or SAW, or by both simultaneously. Since SAW activation can work in a transmission mode, this test structure is also capable of performing SAW sensing of EWOD transported fluidic samples when the EWOD array is located between a pair of SAW IDTs [Fig. 2(b)].

B. SAW IDT Structure Design Considerations

The important design parameter for a SAW device is the IDT finger width d, which determines the resonant frequency f for a given substrate material by

$$f = \frac{v_{SAW}}{\lambda} \tag{1}$$

where $\lambda = 4d$ is the SAW wavelength and v_{SAW} is the sound velocity of the substrate [3].

Clearly, it is important to be able to determine the performance of SAW devices with high resonant frequencies, as these have increased sensitivity when using the technology in the sensing mode.

The IDT finger length sets the width, W, of the SAW wave, which determines the size of a droplet that can be driven by a single IDT. For the SAW elements of the test structures the following design parameters were used: d = 4, 8, 16, 32 μm, W = 200, 500, 1500, 2500, 5000, 7500 μm, and the number of fingers N = 15, 30, 60, 90.

C. EWOD Electrode Design

The EWOD electrode size controls the droplet size that can be held and transported on an EWOD array. It also determines the position at which droplets will be held relative to the IDT, which will affect the mixing motion resulting from SAW activation. For the test structure shown in Fig. 2(a), the electrodes were 1500×1500 μm, and 1000×1000 μm for the structure in Fig. 2(b). In each case, the electrode separation was 10 μm.

The purpose of the electrodes was to perform the normal EWOD functions and also to act as an anchor for droplet during SAW mixing. The distance D between EWOD array and SAW IDTs and the SAW IDT aperture length W were varied in order to determine the maximum power that could be used for mixing before the SAW provides the droplet with sufficient energy to escape from the hydrophilic surface created by the EWOD electrode.

In most cases the sheet resistance of the conducting layer that forms the EWOD electrodes does not significantly affect their performance. However, this is not the case for SAW and so both Ta and Al based test structures were fabricated in order to characterize the effect.

III. Test Structure Fabrication and Characterization Systems

The substrate initially selected for the test structure characterization was 128°-Y-cut $LiNbO_3$, which is readily available.

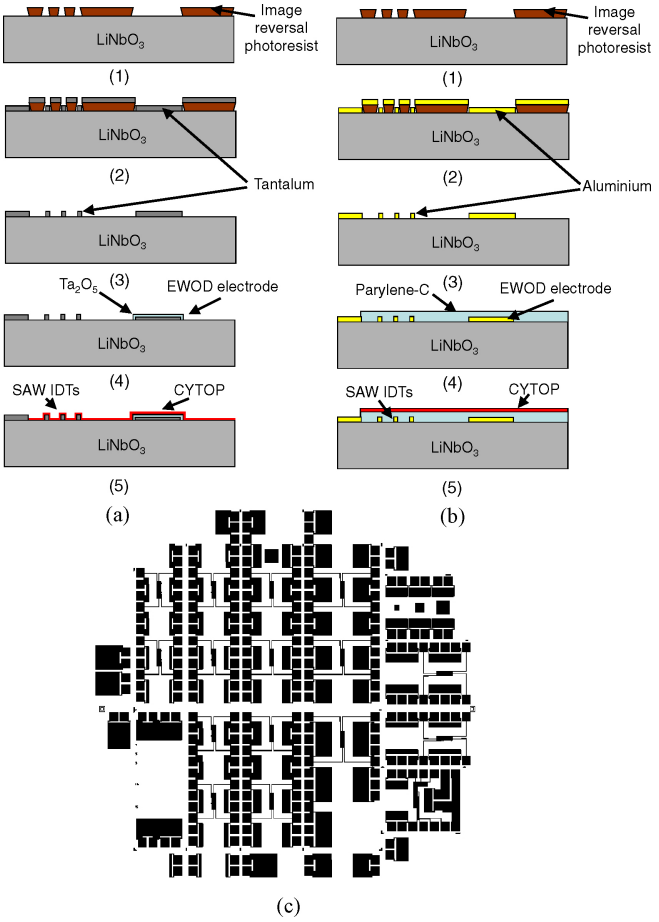

Fig. 3. (a) Process flow of anodic Ta_2O_5 technology based test structures. (b) Process flow of aluminum electrode-based test structures. (c) Layout of test structure mask.

A. Test Structure Fabrication

Metals such as Al and Au are commonly used for SAW IDT electrode fabrication due to their low sheet resistances. For fabricating EWOD electrodes covered by dielectric layers on a piezoelectric substrate such as $LiNbO_3$, high temperature processing is potentially problematic due to its pyroelectric effect [9] and so low temperature processes are preferred to help avert any issues with substrate cracking and breakage.

Room temperature anodic Ta_2O_5 technology [5], [9] was initially selected as the dielectric as this has been successfully used to fabricate low voltage EWOD devices. The aluminum electrode with parylene-C dielectric process was also used for employing aluminum's relatively low sheet resistance. Hence, either tantalum or aluminum was used for both the SAW and EWOD electrodes of the test structures. Fig. 3(a) and (b) shows the process flows of the first reported integrated EWOD-SAW devices which are described in detail in [1]. The electrodes are defined using a lift-off process. The fabrication starts by spinning image reversal (negative) photoresist AZ5214E onto the lithium niobate substrate to act as the sacrificial layer. The resist is patterned using the mask shown in Fig. 3(c) and then developed to leave a negative image of the electrode array. Fig. 3(a) shows that in low voltage EWOD SAW test structures, tantalum is then deposited and

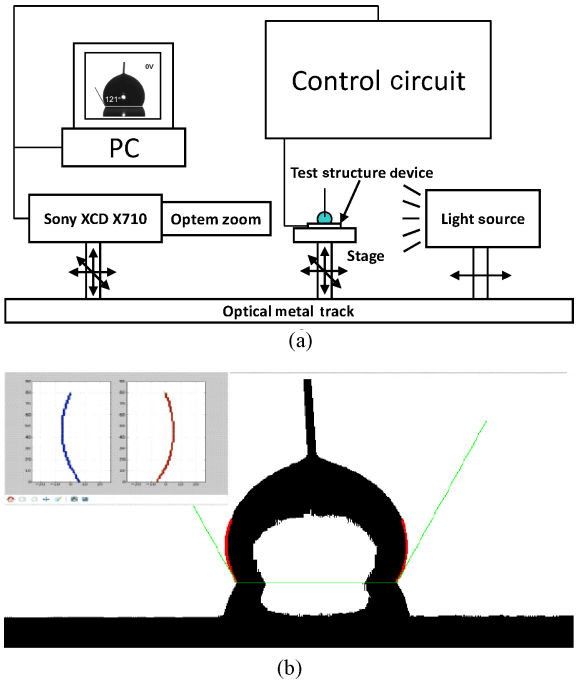

Fig. 4. Characterization system for EWOD SAW integration test structures. (a) EWOD contact angle measurement system with control and image capture units. (b) Screenshot from the contact angle analysis image processing software.

following lift-off, which removes the resist and excess metal, the electrodes are anodized to form the dielectric layer. On top of this, a 20 nm layer of hydrophobic CYTOP is finally spin-coated and cured [9]. Fig. 3(b) shows that a similar fabrication procedure was used to fabricate devices using aluminum for the IDT, with either 0.5 μm parylene or 1 μm parylene together with 20 nm CYTOP dielectric layers on top.

B. Characterization Systems

The EWOD and SAW functions have been first characterized separately on the integration test structures, followed by both separate and combined microfluidic function demonstrations.

1) *EWOD Characterization System:* The performance of EWOD devices depends upon their ability to switch the surface from hydrophobic to hydrophilic by modifying the contact angle (CA) [9]. Hence, a quantified study of the change of the CA has been used to characterize the EWOD performance on the SAW EWOD integration test structures. The CA change can be affected by the EWOD dielectric layer quality, the substrate roughnesses, and evaporation caused by surface heating.

The EWOD function characterization system shown in Fig. 4(a) is based on a standard goniometer normally used for measuring the contact angle, surface energy and surface tension of droplets sitting on a solid surface. In this system, the EWOD voltage applied to the test structure is generated by a fast digital-analog converter with a buffer amplifier in the control unit, which also triggers a CCD camera to capture a single frame each time the EWOD test structure switches. This approach significantly reduces the number of video frames

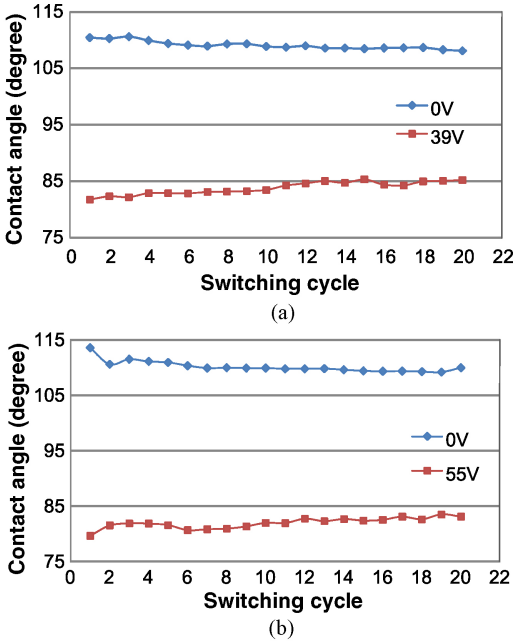

Fig. 5. Contact angle change variation during 20 EWOD switching cycles on $LiNbO_3$ substrates with aluminum electrodes covered by (a) 0.5 μm parylene + 20 nm CYTOP sample using 39V DC, and (b) 1 μm parylene + 20 nm CYTOP sample using 55V DC.

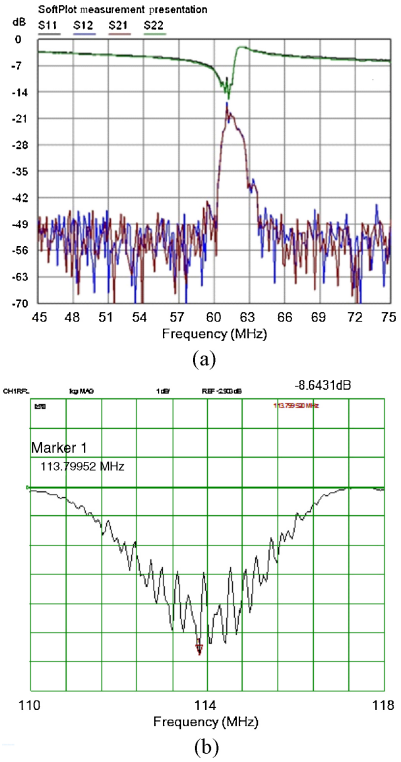

Fig. 6. RF frequency spectrum for SAW devices (N = 30, W = 2500 μm). (a) Reflection and transmission spectrum (d = 16 μm) indicates resonance is being achieved on the integrated device (x-axis: 3 MHz per div). (b) Reflection spectrum on d = 8 μm devices (x-axis: 0.8 MHz per div).

analysed and simplifies the automation of the contact angle extraction. The system runs fully automatically requiring only the data for the number of cycles for the characterization, the timing parameters and the voltage pattern (e.g., a DC voltage pulse) that is applied to the EWOD electrode when being switched. Additionally, the system monitors ambient parameters including temperature and humidity, which should ideally be kept constant to ensure repeatable results [10]. Fig. 4(b) shows the captured images from which the video frames are then analyzed by edge detection image processing software to extract the contact angle readings in switching cycles.

2) *SAW Characterization System:* SAW resonator devices are normally characterized by measuring their resonant frequencies. These frequencies can be affected by the sheet resistance of the metal electrodes and the surface conditions such as the topology. Therefore, the reflection and transmission frequency spectrums of the SAW devices on the EWOD-SAW integration test structures were measured and recorded using a HP-8510 network analyzer.

3) *Fluidic Function Test System:* After the above characterization, the test devices were then used to evaluate fluidic functions. The fluidic functions performed on the SAW-EWOD integration test structure was observed by a computer based microscopic video recording system.

IV. Experiments and Results

A. EWOD Characterization

The devices were initially tested to confirm that EWOD activation was achievable on the integration test structures fabricated on $LiNbO_3$ substrate. Next, contact angle change and switching lifetime test were performed. Fig. 5 shows the EWOD performance life time results for aluminum electrodes covered by (a) 0.5 μm parylene or (b) 1 μm parylene together with 20 nm CYTOP using different DC voltages. The CA change in the initial 20 switching cycles remains above 20° and is very similar to the results on silicon substrates reported in [10] (20° is typically sufficient for repeatable EWOD droplet movement). This result confirms, as would be expected, that EWOD technology performs in a very similar manner on both silicon and $LiNbO_3$ substrates.

B. SAW Characterization

The devices with finger widths between 8 and 16 μm exhibited a good resonance response as shown in Fig. 6. This has been further confirmed by the microfluidic tests detailed below. However, high frequency devices with finger widths of 4 μm only exhibited resonance on the aluminum structures, and not on the tantalum. The reason for this is due to the high sheet resistance of the 300 nm Ta (~8 $\Omega/\square$) used in the structures. This value compared with the 200 nm Al is considerably higher (~0.3 $\Omega/\square$ for sputtered Al).

When moving or mixing with SAW technology, the force exerted on the droplet is not just in the direction of the wave; there is also a component normal to the surface and this can be observed as the droplet "sits up" when the SAW power is initially switched on at a low level. Fig. 7 shows the high degree of droplet distortion that can be achieved when the power is increased. Clearly, the droplet is almost at the stage of

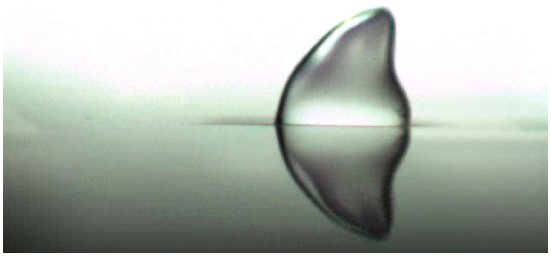

Fig. 7. Droplet being moved toward the right by SAW—any increase in power will cause the droplet to be ejected.

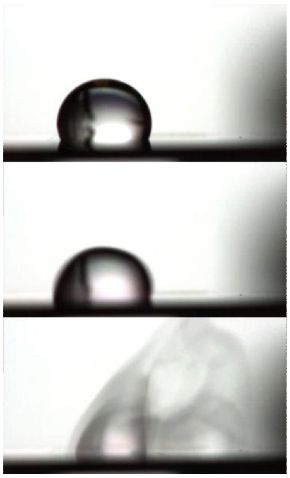

Fig. 8. Three frames from a video showing a droplet being ejected by SAW energy.

being ejected and characterising the power required to instigate this action is important, as is the minimum power required to initiate droplet movement. Fig. 8 shows droplet ejection when the SAW power exceeds the critical maximum power input on the same IDT as in Fig. 7. In this case, instead of moving the droplet along the substrate, it is ejected.

C. Separate Functions on an Integrated Device

Fig. 9 shows examples of test structures fabricated with both EWOD and SAW elements. The photo sequences illustrate the structures successfully demonstrating a capability to manipulate droplets using EWOD and SAW activation. In this structure, the DC voltage required for EWOD activation was around 15 V for Ta/Ta_2O_5/CYTOP devices and 60 V for Al/parylene/CYTOP devices. The SAW input RF powers on the $LiNbO_3$ substrates ranged between 3 dBm (0.1 W) and 30 dBm (1 W) at a frequency of approximately 57 MHz (when the SAW was propagated along the y-axis) and 61.5 MHz (when along the x-axis), for test structures with IDT finger widths of 16 μm, and 114 MHz (y-axis) and 123 MHz (x-axis) for $d = 8\,\mu$m.

D. Combined Microfluidic Functions

Fig. 10 shows SAW induced mixing through the motion of meso-scale (100 μm) silicon cubes inside a droplet that has been held in position by the EWOD electrode array. This is perhaps one of the most important capabilities of EWOD and

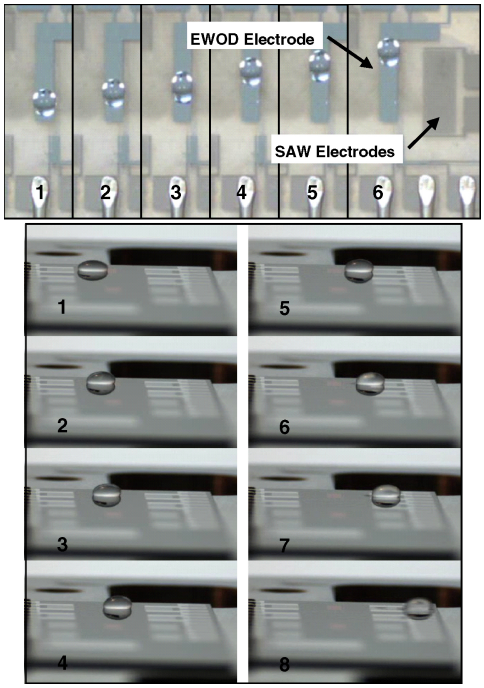

Fig. 9. Time sequence shots of microfluidic droplet on the test chip being moved by EWOD (top) and SAW (bottom).

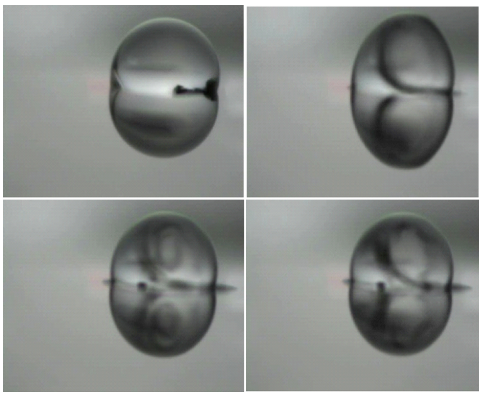

Fig. 10. Four sequential side view photos of 100 μm silicon cubes being mixed inside a DI water droplet using SAW activation while being held in place by EWOD.

SAW integration as it enables droplets to be easily held while performing mixing.

Fig. 11 shows the detailed steps of this function. First, the droplet is positioned at the EWOD electrode centered in front of the SAW IDT, as shown in Fig. 11(a). A d.c. voltage is applied to the two side-electrodes with the central electrode grounded, making it hydrophilic while surrounded by a hydrophobic area. This anchors the droplet while the SAW power is applied for mixing [Fig. 11(c)].

E. Characterization of Combined Microfluidic Functions

The relationship between the applied EWOD voltage and the droplet-displacing SAW transportation force (the power applied to the IDT) for different EWOD/SAW designs has been characterized using the test structures of Fig. 2(a). Fig. 12 shows the results for different SAW IDT apertures W, with the

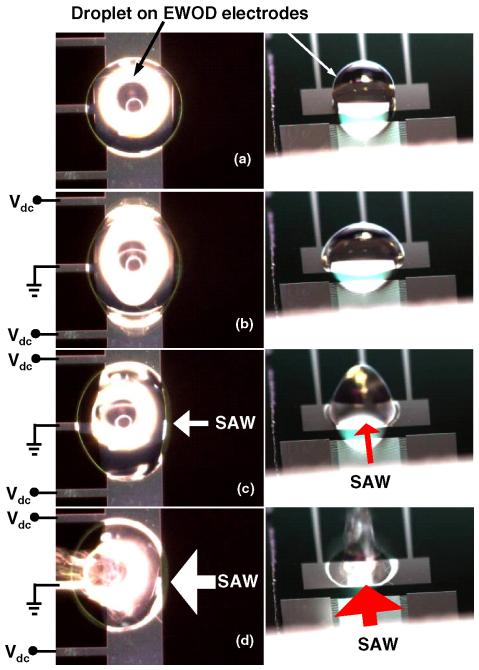

Fig. 11. Test structure shown in Fig. 2(a). Top view (left) and angled view showing the SAW IDT at the bottom of the frames (right). The photographic frames show the sequence of a combined function of SAW and EWOD test structure. (a) Droplet positioned on the central electrode. (b) Droplet held in position by EWOD force. (c) SAW starts in-droplet mixing. (d) Increased SAW power ejects the droplet.

IDT electrode width $d = 16\,\mu$m and the pair number $N = 30$. The EWOD electrode was $1500\times1500\,\mu$m and the EWOD-SAW distance, D, was $3216\,\mu$m.

The maximum power applied to move the droplet forward on the SAW IDTs was 26 dBm, at which point the current flow reaches the 2 A compliance on 200 and $500\,\mu$m IDT aperture devices which have a smaller interdigitated capacitance. Fig. 12 reveals that less EWOD force is required to hold a droplet when the SAW IDT aperture W is reduced. When the SAW IDT aperture W is 0.2 mm, the droplet cannot be displaced by SAW even when the maximum power is applied. Similarly, with a fixed W, increasing the EWOD voltage enables the droplets to be held when larger SAW powers are applied, which, in turn, enables more powerful mixing to be undertaken. The only exception is when $W = 2.5$ mm and the EWOD voltage is 20 V. In this case, the SAW power required to move the droplet reduces to 20 dBm. The reason for this is that the droplet dimension, which is determined by the EWOD electrode size, is smaller than W, meaning the droplet experiences a larger portion of the SAW power as the EWOD force stretches the width of the droplet on the SAW wave path.

Additionally, Fig. 13 shows the effect of the distance D between the SAW IDTs and the EWOD electrode array on the SAW EWOD combined mixing function. When the distance D is reduced from $3216\,\mu$m to $656\,\mu$m, more SAW power is required to displace the droplet held by the same EWOD voltage when $W = 2.5$ mm. This phenomenon is most likely related to surface acoustic wave divergence, making the width of the wave more narrow. This results in the two edges of the

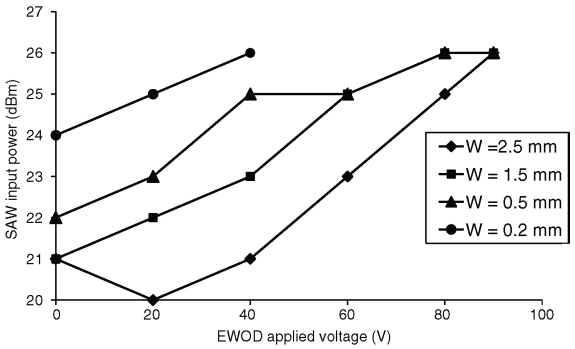

Fig. 12. Relationship between applied EWOD voltages and droplet-displacing SAW power (forward force) in SAW/EWOD test structures with different IDT aperture length W.

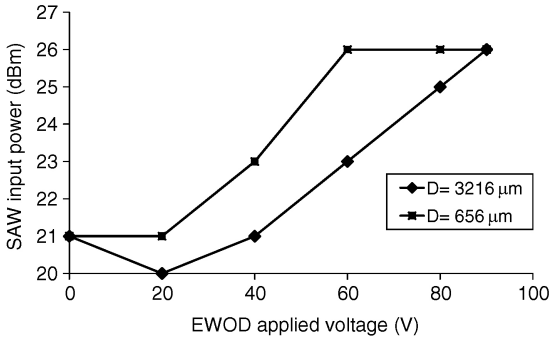

Fig. 13. Relationship between applied EWOD voltages and droplet-displacing SAW powers (forward force) in SAW/EWOD test structures with different SAW/EWOD distance D, when $W = 2.5$ mm.

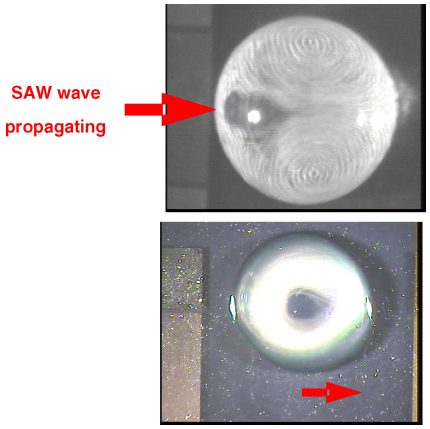

Fig. 14. Different internal mixing stream patterns related to droplet position. Droplet in the central region of the SAW (left). Droplet at one edge of the SAW.

droplet anchored by the EWOD force, experiencing a smaller portion of the SAW power.

F. Other Combined Microfluidic Functions

The mixing pattern exerted on the droplet depends upon whether it is in the center or the edge of the propagating SAW. Fig. 14 shows droplets at different positions in the propagating wave and it can be observed that different mixing stream patterns can be achieved as the droplet is moved from the center to the edge of the wave.

V. Conclusion

This paper presented test structures for the characterization of EWOD and SAW integration. Results demonstrated that a low voltage anodic Ta_2O_5 EWOD process can be integrated with SAW devices. The test structures were used to demonstrate integrated microfluidic functions, and showed that EWOD can successfully anchor a droplet as SAW mixing power was increased. This enabled the maximum power that can be applied to the SAW IDT to be increased, while the droplet was held in position. The characterization also showed that the SAW IDT aperture *W* was also important and needed to be designed ensuring that the EWOD electrodes were suitably placed should mixing or concentration functions be required. Combined microfluidic functions, such as different SAW mixing patterns resulting from different droplet positions, were reported. Future work will involve modeling the surface acoustic waves in the integrated system to understand the wave propagation and divergence, and so on. Other applications, such as SAW sensing on EWOD electrodes, SAW particle concentrating by controlled droplet positioning using EWOD [11], will be explored in more detail.

References

[1] Y. Li, B. W. Flynn, W. Parkes, Y. Liu, Y. Feng, A. D. Ruthven, J. G. Terry, L. I. Haworth, A. Bunting, J. T. M. Stevenson, S. Smith, P. Bobbili, Y. Q. Fu, and A. J. Walton, "The integration of EWOD and SAW technologies for improved droplet manipulation and mixing," in *Proc. ESSDERC*, 2009, pp. 371–374.

[2] R. B. Fair, "Digital microfluidics: Is a true lab-on-a-chip possible?" *Microfluid Nanofluid*, vol. 3, pp. 245–281, Mar. 2007.

[3] A. Wixforth, "Acoustically driven programmable microfluidics for biological and chemical applications," *J. Assoc. Lab. Autom.*, vol. 11, no. 6, pp. 399–405, 2006.

[4] S. K. Cho, H. Moon, and C.-J. Kim, "Creating, transporting, cutting, and merging liquid droplets by electrowetting-based actuation for digital microfluidic circuits," *J. Microelectromech. Syst.*, vol. 12, no. 1, pp. 70–80, 2003.

[5] Y. Li, W. Parkes, L. I. Haworth, A. A. Stokes, K. R. Muir, P. Li, A. J. Collin, N. G. Hutcheon, R. Henderson, B. Rae, and A. J. Walton, "Anodic Ta_2O_5 for CMOS compatible low voltage electrowetting-on-dielectric device fabrication," *Solid-State Electron.*, vol. 52, no. 9, pp. 1382–1387, 2008.

[6] T. Frommelt, M. Kostur, M. Wenzel-Schafer, P. Talkner, P. Hanggi, and A. Wixforth, "Microfluidic mixing via acoustically driven chaotic advection," *Phys. Rev. Lett.*, vol. 100, p. 034502, 2008.

[7] J. K. Luo, Y. Q. Fu, Y. Li, X. Y. Du, A. J. Flewitt, A. J. Walton, and W. I. Milne, "Moving-part-free microfluidic systems for lab-on-a-chip," *J. Micromech. Microeng.*, vol. 19, p. 054001, 2009.

[8] Y. Li, Y. Fu, B. Flynn, W. Parkes, Y. Liu, S. Brodie, J. Terry, L. Haworth, A. Bunting, J. Stevenson, S. Smith, and A. Walton, "Test structures for characterizing the integration of EWOD and SAW technologies for microfluidics," in *Proc. ICMTS*, 2010, pp. 52–57.

[9] Y. Li, W. Parkes, L. I. Haworth, A. W. Ross, J. T. M. Stevenson, and A. J. Walton, "Low voltage electro-wetting on dielectric (EWOD) using CMOS compatible ultrathin amorphous fluoropolymer (aFP) and anodic tantalum pentoxide layers," *J. MEMS*, vol. 17, pp. 1481–1488, 2008.

[10] D. Gruber, Y. Li, S. Smith, A. Tiwari, F. Deng, A. Stokes, J. Terry, A. Bunting, L. Mackay, P. Langridge-Smith, and A. Walton, "Test structures and a measurement system for characterizing the lifetime of EWOD devices," in *Proc. ICMTS*, 2011, pp. 80–84.

[11] Y. Li, Y. Fu, D. Brodie, M. Alghane, and A. J. Walton, "Enhanced micro-droplet splitting, concentration, sensing and ejection by integrating electrowetting-on-dielectrics and surface acoustic wave technologies," in *Proc. Transducers*, 2011, pp. 2936–2939.

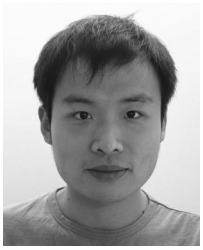

Yifan Li (S'05–M'08) was born in Jiangxi, China, in 1981. He received the B.S. degree from the School of Electrical and Electronics, Shanghai Jiao Tong University, Shanghai, China, in 2003, and the Ph.D. degree from the School of Engineering and Electronics, University of Edinburgh, Edinburgh, U.K., in 2007.

He is currently a Post-Doctoral Researcher with the University of Edinburgh. His current research interests include lab-on-a-chip, self-assembly, and biomicroelectromechanical system technologies.

Dr. Li has been a member of IET (was known as IEE) since 2005.

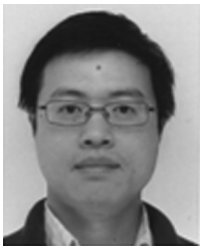

Richard Yongqing Fu (M'07) is currently a Reader with the Thin Film Centre, University of the West of Scotland, Paisley, U.K.

He has published about 150 SCI journal papers and two books. His current research interests include microactuators, microsensors, and microfluidic devices based on smart functional thin film materials.

D. Winters, photograph and biography not available at the time of publication.

Brian W. Flynn was born in Edinburgh, U.K., in 1949. He received the B.Sc. and Ph.D. degrees in electrical engineering from the University of Edinburgh, Edinburgh.

He is currently a Senior Lecturer with the Department of Electrical Engineering, University of Edinburgh. His current research interests include machine wear debris monitoring using inductive sensors and wireless power transfer.

Dr. Flynn is a member of the Institution of Engineering Technology and a Chartered Engineer in the U.K.

Bill Parkes has spent a number of years working on the development of microfabrication techniques based on a range of aspects of silicon technology. The notable devices produced include structures for submillimeter imaging detectors, thin membrane pressure sensors, focusing x-ray micromirrors, and microarray chambers for bioanalysis.

Douglas Stuart Brodie received the Bachelors degree in mechanical engineering from Heriot-Watt University, Edinburgh, U.K., in 2001, where he is currently pursuing the Ph.D. degree in surface acoustic wave microfluidics.

He was involved in the industry for many years before returning to academia in 2009. His current research interests include surface acoustic waves, microfluidics, and coupled acoustic fluidic finite element modeling.

Mr. Brodie is a member of the IMechE, the Institute of Mechanical Engineers.

Yufei Liu received the B.Sc. degree in physics and the B.A. degree in economics from Peking University, Beijing, China, in 2003, the M.Eng. degree from the Chinese Academy of Sciences, Beijing, in 2006, and the Ph.D. degree from Heriot-Watt University, Edinburgh, U.K., in 2011.

He is currently a Research/Knowledge Transfer Officer with the College of Engineering, Swansea University, Swansea, U.K. His current research interests include micro/nano technology, MEMS and optical MEMS, device simulation and fabrication technologies, and photovoltaics.

Jonathan Terry (M'08) received the M.Sc. degree in microelectronic material and device technology and the Ph.D. degree in solid state electronics from the Institute of Science and Technology, University of Manchester, Manchester, U.K.

He joined the Institute for Integrated Micro and Nano Systems, University of Edinburgh, Edinburgh, U.K., in 1999 as a Research Fellow. He is currently a Senior Research Fellow with the University of Edinburgh where his interests include the design, fabrication, and optimization of MEMS structures and their integration with CMOS technology. He is a Lead Researcher with the Smart Microsystems Research Consortium and runs courses on microfabrication techniques.

Les I. Haworth received the B.Sc. degree in electronics and the Ph.D. degree in semiconductor materials from the University of Salford, Salford, U.K., in 1976 and 1985, respectively.

He has been with Ferranti Electronics, Ltd., Edinburgh, U.K., as a Production Fabrication Engineer. He has been with the University of Edinburgh, Edinburgh, since 1987, as a Lecturer. His current research interests include silicon wafer fabrication, including the formation of refractory metal silicides by ion beam mixing, and the development of rapid thermal processing equipment and processes. Currently, he is conducting research on impurity gettering in devices, MEMS fabrication, and microfluidics.

Dr. Haworth is a member of the Institution of Engineering and Technology, U.K., and a fellow of the Higher Education Academy.

A. S. Bunting, photograph and biography not available at the time of publication.

J. T. M. Stevenson, photograph and biography not available at the time of publication.

Stewart Smith (M'05) received the B.Eng. (Hons.) degree in electronics and electrical engineering and the Ph.D. degree from the University of Edinburgh, Edinburgh, U.K., in 1997 and 2003, respectively.

He is currently an RCUK Academic Fellow with the School of Engineering, University of Edinburgh. His current research interests include the design and fabrication of biomedical microsystems, test structures for MEMS processes, and the electrical characterization of advanced photomasks.

Dr. Smith is a member of the Technical Committee for the IEEE International Conference on Microelectronic Test Structures.

C. Logan Mackay, photograph and biography not available at the time of publication.

Pat R. R. Langridge-Smith is currently a Reader in chemical physics with the University of Edinburgh, Edinburgh, U.K., and the Founder and Director of the Scottish Instrumentation and Resource Centre for Advanced Mass Spectrometry (SIRCAMS), School of Chemistry, University of Edinburgh. A unifying theme of the research from his group, the Exploratory Measurement Science Group, is the use of the most advanced mass spectrometric instrumentation, together with miniaturized techniques for sample handling and microseparation, to address important areas of measurement science. This has included a collaboration with HD Technology, Ltd., Manchester, U.K., which eventually led to the development of the orbitrap mass spectrometer, now marketed by Thermo Scientific, Bremen, Germany.

Dr. Langridge-Smith was elected as a fellow of the Institute of Physics in 2000.

Adam A. Stokes (M'06) received the B.Eng. (Hons.) degree in electronics and electrical engineering from the University of Edinburgh, Edinburgh, U.K., in 2006, the M.Res. degree in biomedical science from the University of Glasgow, Glasgow, U.K., in 2007, and the Ph.D. degree in physical chemistry and microelectronic engineering from the University of Edinburgh, in 2010.

He is currently a fellow with the Laboratory of Professor George M. Whitesides, Harvard University, Cambridge, MA. His current research interests include proteomics and mass spectrometry, chemistry and chemical biology, droplet microfluidics, unconventional micro/nano fabrication, optical metamaterials, electromagnetics, control theory, robotics, and soft-robotics.

Anthony J. Walton (M'88–SM'09) is currently a Professor of microelectronic manufacturing with the School of Engineering and Electronics, University of Edinburgh, Edinburgh, U.K. He has been actively involved with the semiconductor industry in a number of areas associated with silicon processing that includes both integrated circuit technology and microsystems over the past 25 years. He has published over 300 papers.

He has received Best Paper Awards from the IEEE TRANSACTIONS ON SEMICONDUCTOR MANUFACTURING, Proc ISHM, and IEEE ICMTS 2004, as well as the IET Nanobiotechnology 2007 IET Premium Paper Award.